

# A combined experimental and density functional study of 1-(arylsulfonyl)-2-*R*-4-chloro-2-butenes reactivity towards the allylic chlorine

Sergey V. Bondarchuk<sup>a\*</sup>, Victor V. Smalius<sup>a</sup> and Boris F. Minaev<sup>a,b</sup>

Nucleophilic substitution and dehydrochlorination reactions of a number of the ring-substituted 1-(arylsulfonyl)-2-*R*-4-chloro-2-butenes are studied both experimentally and theoretically. The developed synthetic procedures are characterized by a general rapidity, cheapness, and simplicity providing moderate to high yields of 1-arylsulfonyl 1,3-butadienes (48–95%), 1-(arylsulfonyl)-2-*R*-4-(*N,N*-dialkylamino)-2-butenes (31–53%), 1-(arylsulfonyl)-2-*R*-2-buten-4-ols (37–61%), and bis[4-(arylsulfonyl)-3-*R*-but-2-enyl]sulfides (40–70%). The density functional theory B3LYP/6-311++G(2d,2p) calculations of the intermediate allylic cations in acetone revealed their high stability occurring from a resonance stabilization and hyperconjugation by the SO<sub>2</sub>Ar group. The reactivity parameters estimated at the bond critical points of the diene/allylic moiety display a high correlation ( $R^2 > 0.97$ ) with the Hammett ( $\sigma_p$ ) constants. 1-Arylsulfonyl 1,3-butadienes are characterized by a partly broken  $\pi$  conjugated system, which follows from analysis of the two-centered delocalization ( $\delta$ ) and localization ( $\lambda$ ) index values. The highest occupied molecular orbital energies of 1-arylsulfonyl 1,3-butadienes are lower than those of 1,3-butadiene explaining their low reactivity towards the Diels–Alder condensation. Copyright © 2015 John Wiley & Sons, Ltd.

**Keywords:** 1-(arylsulfonyl)-2-*R*-4-chloro-2-butenes; 1-arylsulfonyl 1,3-dienes; conceptual density functional theory; electrophile-nucleophile interactions; quantum theory of atoms in molecules

## INTRODUCTION

Recently, a renewed growing interest is observed towards the synthetic capabilities of 1-(arylsulfonyl)-2-*R*-4-chloro-2-butenes (**1a–1j**). This is because of their use in the synthesis of coenzyme Q<sub>10</sub><sup>[1,2]</sup> and of highly functionalizable 1-arylsulfonyl 1,3-dienes.<sup>[3–10]</sup> The 4-chloro-2-methyl-1-phenylsulfonyl-2-butene species is an intermediate in the synthesis of coenzyme Q<sub>10</sub><sup>[1,2,11]</sup> and the latter dienes were found to react efficiently with aryl diazonium salts at the 3 and 4 positions.<sup>[3–10,12,13]</sup> A further dehydrochlorination of this reaction product will result in the formation of a more complex diene and so on. As it follows from our present unpublished results, these dienes are efficient rubber additives for car tires increasing adhesion to the tire cord. Meanwhile, the studied butenes possess effective herbistatic properties against *Echinochloa crus-galli* L., *Amaranthus retroflexus* L., and *Chenopodium album* L. at typical concentrations of 0.1–0.001%.

In contrast to the mentioned butenes, the 2-arylsulfonyl 1,3-dienes, 1,3-bis(arylsulfonyl) 1,3-dienes and, especially, 2,3-bis(arylsulfonyl) 1,3-diene compounds are studied much better.<sup>[14,15]</sup> In two recent exhaustive reviews, Flick and Padwa described a broad variety of syntheses towards azapolycyclic ring systems and piperidone derivatives.<sup>[16,17]</sup> One should note that the molecules containing the arylsulfonyl moiety are well known as physiologically active compounds, for example, sulfonamide drugs. The recent pharmacological evaluations, however, reveal that the other arylsulfonyl-containing molecules – very different structurally – also possess biological activity. In particular, 1-aryloxy(1-arylsulfonyl)-4-bis(trifluoromethyl)alkyl semicarbazides,<sup>[18]</sup>

2-(methylaminosulfonyl)-1-(arylsulfonyl)hydrazines,<sup>[19]</sup> 1-(sulfonyl)-5-(arylsulfonyl)indoline,<sup>[20]</sup> *N*-arylsulfonyl-*N*-methyl-*N'*-(2,2-dimethyl-2*H*-1-benzopyran-4-yl)ureas<sup>[21]</sup>, and aryl sulfonyl fluorides<sup>[22]</sup> were successfully evaluated as myorelaxants and anticancer agents. Thus, we suspect that the products of S<sub>N</sub> reactions of 1-(arylsulfonyl)-2-*R*-4-chloro-2-butenes with the studied nucleophiles might be predicted as biologically active compounds.

As a synthetic route to yield 1-(arylsulfonyl)-2-*R*-4-chloro-2-butenes the Asscher–Vofsi reaction is usually applied.<sup>[2]</sup> Another method leading to a broad variety of 1-(arylsulfonyl)-2-*R*-4-chloro-2-butenes is represented as the Michael addition of nucleophiles to 1-arylsulfonyl 1,3-dienes.<sup>[15,23]</sup> Earlier, we have developed an alternative method for preparing 1-(arylsulfonyl)-2-*R*-4-chloro-2-butenes using arylation of conjugated dienes with aryl diazonium salts in the SO<sub>2</sub> saturated solution.<sup>[3–13]</sup> In contrast to the previously developed methods, this protocol is very simple, relatively fast, and does not need expensive reactants or catalysts.<sup>[2,15,23]</sup>

\* Correspondence to: S. V. Bondarchuk, Department of Organic Chemistry, Bogdan Khmelnytsky Cherkasy National University, blvd. Shevchenko 81, 18031 Cherkasy, Ukraine.  
E-mail: bondchem@cdu.edu.ua

<sup>a</sup> S. V. Bondarchuk, V. V. Smalius, B. F. Minaev  
Department of Organic Chemistry, Bogdan Khmelnytsky Cherkasy National University, blvd. Shevchenko 81, 18031, Cherkasy, Ukraine

<sup>b</sup> B. F. Minaev  
Department of Theoretical Chemistry and Biochemistry, Royal Institute of Technology, AlbaNova, S-106 91, Stockholm, Sweden

1-(Arylsulfonyl)-2-*R*-4-chloro-2-butenes and 1-arylsulfonyl 1,3-dienes are also interesting compounds from theoretical point of view. The former contains a strong electron-withdrawing (ArSO<sub>2</sub>) group and the allylic chlorine atom. Therefore, their S<sub>N</sub> reactions are expected to be rather efficient. On the other hand, 1-arylsulfonyl 1,3-dienes possess the conjugated π system, which is bound with the ArSO<sub>2</sub> group. Thus, their reactivity towards the Diels–Alder or polar addition is of special current interest.<sup>[24–29]</sup> In order to study the influence of the latter group, we have performed a series of S<sub>N</sub> reactions of 13 various 1-(arylsulfonyl)-2-*R*-4-chloro-2-butenes with such nucleophiles as diethylamine, diethanolamine, morpholine, potassium hydroxide, and sodium sulfide as well as the dehydrochlorination reaction yielding the corresponding 1-arylsulfonyl 1,3-dienes followed by the Diels–Alder addition with maleic anhydride. Although 1-arylsulfonyl 1,3-dienes are expected to match better in the inverse electron demand Diels–Alder reaction, we have selected maleic anhydride as a dienophile because the latter yields crystalline adducts, which are used for the diene identification by characteristic melting points.

In the present study, the reactivity parameters of the studied compounds and the reactive intermediates have been determined in terms of conceptual density functional theory (DFT). Because the S<sub>N</sub> reactions are generally described as electrophile–nucleophile interactions, the Mayr–Patz equation<sup>[30–33]</sup> has been applied to estimate the corresponding reaction rate. Recently, we have examined this method for the aryl cations reactions with π-nucleophiles and have approved its reliability.<sup>[34–36]</sup> A rationale of the dependence between the reaction rates and isolated yields has been proposed on the ground of the obtained log *k* values. Meanwhile, the topological analysis of the electron density and the global/local electronic structure descriptors has enabled us to explain peculiar reactivity of 1-arylsulfonyl 1,3-dienes towards addition reactions.

Although some of the presented reactions are not principally new,<sup>[15]</sup> we propose synthetic procedures that are much faster, cheaper, and simpler than the previously developed synthesis. The described computational approach will be useful for studying chemical reactivity in the electrophile–nucleophile reactions of 1-(arylsulfonyl)-2-*R*-4-chloro-2-butenes, 1-arylsulfonyl 1,3-dienes, and the related compounds.<sup>[16,17,37–40]</sup>

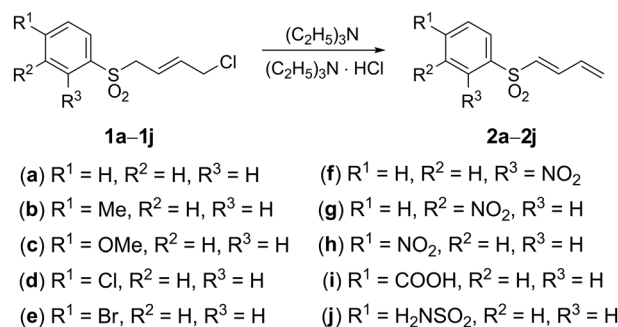
## RESULTS AND DISCUSSION

### Experimental study of the 1-(arylsulfonyl)-2-*R*-4-chloro-2-butenes reactivity

As our experiments revealed, the allylic chlorine atom in 1-(arylsulfonyl)-2-*R*-4-chloro-2-butenes, containing different substituents at the ortho, meta, and para positions of the benzene ring, can undergo dehydrochlorination as well as nucleophilic substitution in the reaction with alkylamines, potassium hydroxide, and sodium sulfide. Thus, heating of 1-(arylsulfonyl)-2-*R*-4-chloro-2-butenes with an equimolar amount of triethylamine in a solution of benzene or acetone leads to the elimination of hydrogen chloride and subsequent formation of 1-arylsulfonyl 1,3-dienes **2a–2j** (Scheme 1).

The structures of the sulfonyl-containing dienes **2f** and **2j** have been confirmed using the proton nuclear magnetic resonance (<sup>1</sup>H NMR) spectroscopic analysis. Recorded spectrum of the diene **2j** is illustrated in Fig. S1 in the Supporting Information, and the spectra assignment is discussed in the related text.

Application of DFT, described in the succeeding text, explains the detected NMR spectra pretty well (Table S1 in the Supporting



**Scheme 1.** Formation of 1-arylsulfonyl 1,3-dienes **2a–2j** by dehydrochlorination of 1-(arylsulfonyl)-2-*R*-4-chloro-2-butenes **1a–1j**

Information). We have calculated the nuclear chemical shift according to the following definition:<sup>[41]</sup>

$$\delta = \sigma_{iso}^{TMS} - \sigma_{iso}^{sample} \quad (1)$$

where  $\sigma_{iso}^{sample}$  and  $\sigma_{iso}^{TMS}$  are the values of isotropic shielding for protons in the studied molecule (**2f**) and tetramethylsilane as a reference, respectively. The isotropic shielding is the average of the diagonal elements of the shielding tensor:<sup>[41]</sup>

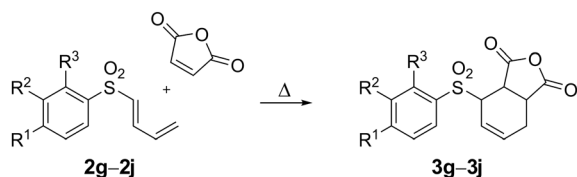
$$\sigma_{iso} = (\sigma_{xx} + \sigma_{yy} + \sigma_{zz})/3 \quad (2)$$

We used the B3LYP/6-311++G(d,p) approach in terms of the gauge-independent atomic orbital method. As it follows from Table S1, the semi-quantitative (qualitative) agreement between calculated and experimental NMR chemical shifts permits us to make definite assignments. The most interesting results concern the aromatic protons assignment in the **2f** species. The proton H(22) (the hydrogen atom labeling is given in Fig. S2 in the Supporting Information) demonstrates the largest low-field chemical shift and is separated from other aromatic protons (probably because of perturbation from the nearby oxygen atom). Our DFT calculation reproduces this peculiarity pretty well, which supports the total reliable NMR assignment.

Our joint researches with the Institute of Macromolecular Chemistry (National Academy of Sciences of Ukraine) have demonstrated that the diene **2h** well copolymerizes with isoprene. The obtained copolymer bears the nitro group in the benzene nucleus; this can increase adhesion to the rubber fillers and tire cord.

Taking into account a significant weakening of the π-conjugation in the dienes **2a–2j**, we have tried to study their reactivity towards the Diels–Alder condensation. It was found that the studied dienes react poorly with maleic anhydride. Heating of the reactants in benzene or xylene in the presence of iodine failed. Only a sustainable melting of equimolar amounts of the dienes **2a–2j** with freshly sublimed maleic anhydride have yielded crystal 1-(arylsulfonyl)-1,4,5,6-tetrahydrophthalic anhydrides **3g–3j** (Scheme 2).

Because of instability of the dienes **2a–2e** at high temperatures, we could not obtain the corresponding adducts. On the other hand, the diene **2f** does not react with maleic anhydride too. This is caused by a strong electron withdrawing effect of the 2-nitro substituent with respect to the conjugated π system of the diene moiety. Such electron depletion is the reason why the dienes **2** do not undergo the Knoevenagel–hetero-Diels–Alder condensation.<sup>[42]</sup> It is worthwhile noting that the energy



**Scheme 2.** The Diels-Alder reaction of the dienes **2** with maleic anhydride

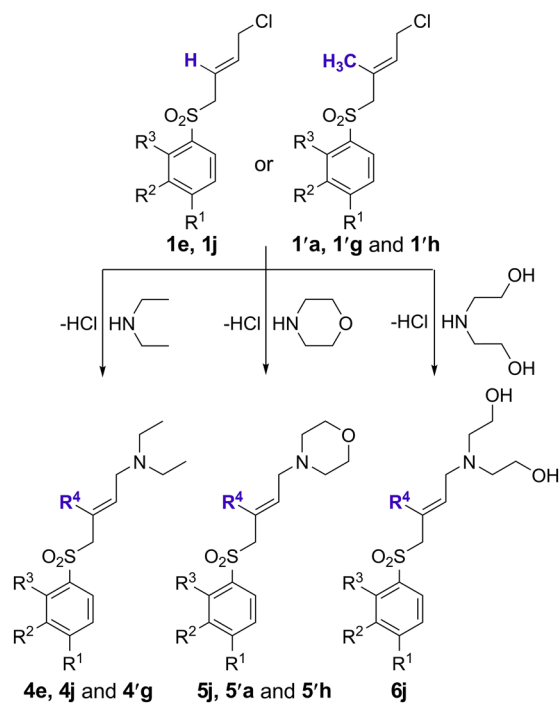
of *cis*-*trans* isomerization of the dienes **2g-2j** are the following: **2g** (3.43 kcal/mol), **2h** (3.45 kcal/mol), **2i** (3.43 kcal/mol), and **2j** (3.45 kcal/mol). Because, these energy values are rather small, these can be easily overcome under the reaction conditions.

The structure of adducts **3g** and **3h** was confirmed by proton nuclear magnetic resonance ( $^1\text{H}$  NMR) spectroscopy. Recorded spectrum of the adduct **3g** is illustrated in Fig. S3 in the Supporting Information, and the spectra assignment is discussed in the related text.

Heating of the acetone solutions of the 1-(arylsulfonyl)-4-chloro-2-butenes **1e** and **1j** ( $R^4 = \text{H}$ ) and 1-(arylsulfonyl)-4-chloro-2-methyl-2-butenes **1'a**, **1'g**, and **1'h** ( $R^4 = \text{CH}_3$ ) with secondary amines leads to sulfonyl-containing fatty-aromatic tertiary amines. Thus, the reactions with equimolar amounts of diethylamine, morpholine, and diethanolamine yield 1-(arylsulfonyl)-2-*R*-4-*N*,*N*-diethylamino-2-butenes (**4e**, **4j**, and **4'g**), 1-(arylsulfonyl)-2-*R*-4-*N*-morpholyl-2-butenes (**5j**, **5'a**, and **5'h**), and 1-(4-sulfamoylphenylsulfonyl)-4-*N*,*N*-hydroxyethyl-2-butene **6j**, respectively (Scheme 3).

The structure of compounds **5'a** and **5'h** was confirmed by means of  $^1\text{H}$  NMR spectroscopy. Recorded spectrum of the compound **5'a** is illustrated in Fig. S4 in the Supporting Information, and the spectra assignment is discussed in the related text.

1-(Arylsulfonyl)-2-*R*-4-chloro-2-butenes (**1g**, **1h**, **1j**, and **1'h**) also undergo hydrolysis to form the corresponding primary



**Scheme 3.** Substitution of the active chlorine atom of the butenes **2** by the diethylamine, morpholine, and diethanolamine moieties

alcohols. Thus, treating an acetone solution of 1-(arylsulfonyl)-2-*R*-4-chloro-2-butene with a 10% water solution of potassium hydroxide yields the corresponding 1-(arylsulfonyl)-2-*R*-2-buten-4-ol (Scheme 4). The obtained alcohols **7** can be reconverted to the initial chlorides **1** up to 90% yield when treating with thionyl chloride (Scheme 4). The results of elemental analysis of the obtained alcohols **7** revealed zero chlorine content.

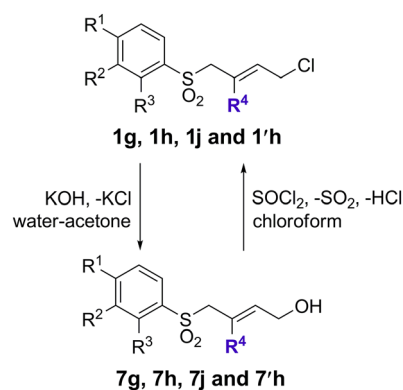
A mixing of 1-(arylsulfonyl)-2-*R*-4-chloro-2-butenes obtained using arylation of 1,3-butadiene and isoprene with aryl diazonium salts in the  $\text{SO}_2$  saturated solution and those obtained according to Scheme 4 has suggested no melting point depression; this justifies an identity of the mixed solids. The corresponding values of melting point of the chlorides **1** can be found elsewhere.<sup>[3-5,13]</sup>

Additionally, 1-(arylsulfonyl)-2-*R*-4-chloro-2-butenes easily react with sodium sulfide to give the corresponding sulfonyl-containing fatty-aromatic sulfides. Thus, when treating an acetone solution of the corresponding butene with a water solution of  $\text{Na}_2\text{S}$ , a nucleophilic substitution of the allylic chlorine in two butene molecules smoothly occurred; this yields bis[4-(arylsulfonyl)-3-*R*-but-2-enyl] sulfides **8g-8j** and **8'h** (Scheme 5).

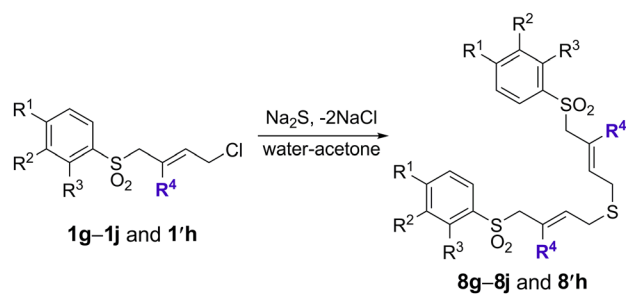
The composition of fatty-aromatic sulfides **8g** and **8h** was determined by the  $^1\text{H}$  NMR spectroscopic analysis. Recorded spectrum of the sulfide **8g** is illustrated in Fig. S5 in the Supporting Information, and the spectra assignment is discussed in the related text.

### Quantum-chemical calculations

The DFT calculations performed within this study have been aimed to explain the peculiarities of reactivity of 1-(arylsulfonyl)-2-*R*-4-



**Scheme 4.** Reversible transformations between 1-(arylsulfonyl)-2-*R*-4-chloro-2-butenes (**1**) and 1-(arylsulfonyl)-2-*R*-2-buten-4-ols (**7**)



**Scheme 5.** Nucleophilic substitution of the allylic chlorine with sodium sulfide yielding bis[4-(arylsulfonyl)-3-*R*-but-2-enyl]sulfides (**8**)

chloro-2-butenes (**1**) as well as 1-arylsulfonyl 1,3-dienes (**2**). Because the nucleophilic substitution of chlorine is accompanied with an intermediate formation of the allylic cations (**1**<sup>+</sup>), the reactivity of the butenes **1** towards S<sub>N</sub> reactions is best described in terms of the Mayr–Patz electrophile quantification scheme.<sup>[30–33]</sup> DFT calculations support the general assumption of the S<sub>N</sub>1 mechanism of the reactions presented in Scheme 1; thus, the rate constant logarithm of the electrophile–nucleophile reaction can be expressed as in Eqn (3)

$$\log k = s(E + N_{\text{exper}}) \propto \omega + N_{\text{ad}} \quad (3)$$

where  $N_{\text{exper}}$  is the relative reactivity,  $E$  is the nucleophile independent electrophilicity parameter, and  $s$  is the empirical parameter.<sup>[30–33]</sup> The experimentally derived parameters  $E$  and  $N_{\text{exper}}$  are proportional to the adiabatic global electrophilicity ( $\omega$ ) and nucleophilicity indexes ( $N_{\text{ad}}$ ).

The former is calculated according to the well-known Parr scheme;<sup>[43]</sup> it includes electron chemical potential ( $\mu$ )<sup>[44]</sup> and chemical hardness ( $\eta$ ).<sup>[45]</sup> Consequently, after simplification, one obtains the following expression:

$$\omega = \frac{(IE - EA)^2}{8(IE - EA)} \quad (4)$$

Herein,  $IE$  and  $EA$  are the adiabatic ionization energy and electron affinity.<sup>[34–36]</sup>

$$IE = U_X^{n+1} - U_X^n = \left( E_{\text{elec}(X)}^{n+1} + ZPVE_X^{n+1} \right) - \left( E_{\text{elec}(X)}^n + ZPVE_X^n \right) \quad (5)$$

$$EA = U_X^n - U_X^{n-1} = \left( E_{\text{elec}(X)}^n + ZPVE_X^n \right) - \left( E_{\text{elec}(X)}^{n-1} + ZPVE_X^{n-1} \right) \quad (6)$$

The adiabatic values are much more accurate than ones obtained within the “vertical” approach.<sup>[34–36]</sup> Finally, the adiabatic nucleophilicity index has been calculated as the following:<sup>[46]</sup>

$$N_{\text{ad}} = 11.79 - IE_{\text{Nu}} \quad (7)$$

Herein,  $IE_{\text{Nu}}$  is the adiabatic ionization energy of the corresponding nucleophile, and the number 11.79 corresponds to the  $IE$  value (in eV) of the tetracyanoethylene molecule as a reference.<sup>[47]</sup>

Thus, we have calculated the  $IE$ ,  $EA$ ,  $\mu$ ,  $\eta$ , and  $\omega$  parameters for the studied allylic cations. The data obtained are listed in Table 1. It is interesting that the  $\omega$  values rise when the corresponding ring substituent possesses the higher electron-donating ability. Moreover, the methyl group in the cations **1**<sup>+</sup> decreases the  $\omega$  values significantly (Table 1). The Hammett constants ( $\sigma_p$ ),<sup>[48]</sup> however, do not correlate with the latter values, but strongly correlate with the  $EA$  values ( $R^2 = 0.9748$ ). The correlation plot is presented in Fig. S6 in the Supporting Information. The absolute values of global electrophilicity index are somewhat lower than those of the singlet and triplet aryl cations (9–21 eV).<sup>[34]</sup> Consequently, one may suspect that S<sub>N</sub> reactions of the allylic cations **1**<sup>+</sup> and **1**<sup>+</sup> are not diffusion controlled. Thus, we have calculated the  $\log k$  values for the products **4–8** because these reactions can be presented as electrophile–nucleophile addition between the studied allylic cations and the corresponding nucleophile.

**Table 1.** Adiabatic ionization energies ( $IE$ ), electron affinities ( $EA$ ), electronic chemical potential ( $\mu$ ), chemical hardness ( $\eta$ ), and global electrophilicity index ( $\omega$ ) of the allylic cations (**1**<sup>+</sup> and **1**<sup>+</sup>) (in eV) calculated at the B3LYP/6-311++G(2d,2p) level of theory in acetone

Entry	$IE$	$EA$	$\mu$	$\eta$	$\omega$
<b>1a</b> <sup>+</sup>	7.73	5.64	−6.69	2.09	10.67
<b>1b</b> <sup>+</sup>	7.51	5.62	−6.56	1.89	11.38
<b>1c</b> <sup>+</sup>	7.02	5.58	−6.30	1.44	13.82
<b>1d</b> <sup>+</sup>	7.66	5.67	−6.66	1.99	11.14
<b>1e</b> <sup>+</sup>	7.56	5.67	−6.61	1.89	11.59
<b>1f</b> <sup>+</sup>	8.07	5.75	−6.91	2.32	10.27
<b>1g</b> <sup>+</sup>	8.24	5.73	−6.99	2.51	9.74
<b>1h</b> <sup>+</sup>	8.19	5.74	−6.97	2.45	9.92
<b>1i</b> <sup>+</sup>	7.92	5.70	−6.81	2.22	10.43
<b>1j</b> <sup>+</sup>	7.92	5.71	−6.82	2.22	10.47
<b>1a</b> <sup>+</sup>	7.71	5.34	−6.53	2.37	8.99
<b>1g</b> <sup>+</sup>	8.23	5.43	−6.83	2.80	8.33
<b>1h</b> <sup>+</sup>	8.20	5.44	−6.82	2.76	8.41

**Table 2.** The calculated  $\log k$  values for the nucleophile–electrophile reactions yielding products **4–8**

Product	$\log k$	Product	$\log k$	Product	$\log k$
<b>4j</b>	16.50	<b>5'a</b>	15.01	<b>7h</b>	16.06
<b>4e</b>	17.61	<b>6j</b>	16.43	<b>8h</b>	17.56
<b>4'g</b>	14.36	<b>7j</b>	16.61	<b>8g</b>	17.39
<b>5j</b>	16.49	<b>7'h</b>	14.55	<b>8i</b>	18.07
<b>5'h</b>	14.43	<b>7g</b>	15.88	<b>8j</b>	18.12

The results are listed in Table 2. The nucleophilicity indexes for the studied reactants, calculated according to Eqn (7), are the following: diethylamine (6.03 eV), morpholine (6.02 eV), diethanolamine (5.96 eV), potassium hydroxide (6.14 eV), and sodium sulfide (7.65 eV), respectively. We should stress that the calculated absolute  $\log k$  values cannot be directly compared with the experimentally obtained values. These can either serve as the semi-quantitative reactivity descriptors or need a calibration with some related reference systems.

In order to check how the calculated  $\log k$  values describe the obtained reaction yield, we have built a plot (Fig. 1). As expected, high  $\log k$  values correspond to the higher yields. Taking into account that a yield equals to zero when  $\log k = 0$ , we have approximated the obtained data with two curves. The red curve (Fig. 1(a)) includes all the product yields, except ones corresponding to the cations **1j**<sup>+</sup> and **1e**<sup>+</sup>. The latter products are better described by another similar function (Fig. 1(b)). This is likely due to some synthetic peculiarities that cannot be accounted within these calculations.

The optimized structure of the cation **1a**<sup>+</sup> is illustrated in Fig. 2, while the structural parameters of all the studied allylic cations are presented in Fig. S7 in the Supporting Information. As it follows from the molecular electrostatic potential (ESP) 3D map, a uniform positive charge delocalization occurs onto the allylic moiety (Fig. 2). Although, an electron depletion, caused by the arylsulfonyl group, results in higher ESP values at the C(2) atom rather than at the C(4), the condensed Fukui function ( $f^+$ ) values

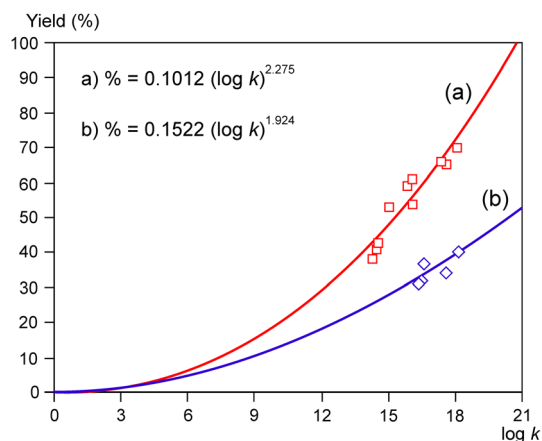


**Figure 1.** Yields of the nucleophilic substitution reactions forming the products **4–8** versus the corresponding reaction rate logarithms ( $\log k$ ) calculated by the Mayr–Patz equation

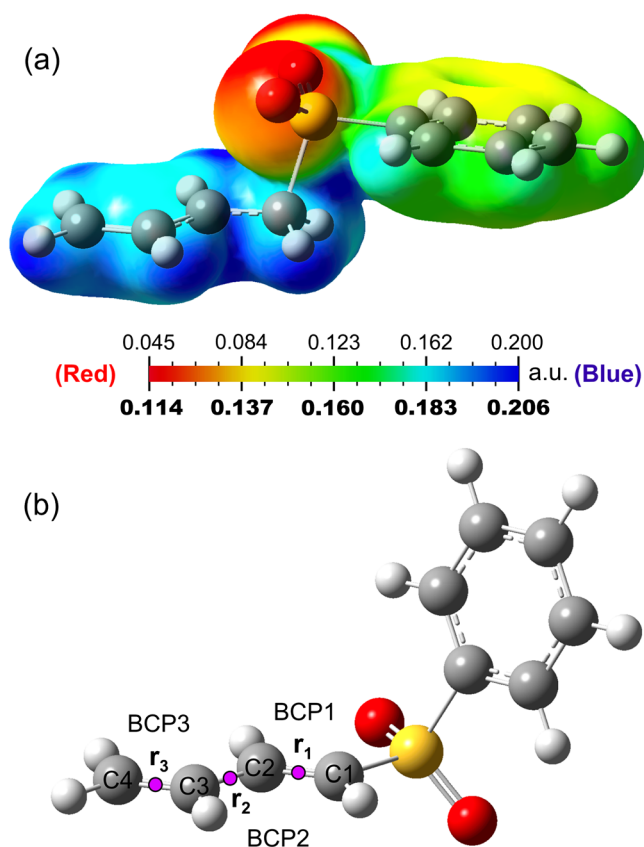


**Figure 2.** The structure of the cation **1a<sup>+</sup>** together with molecular electrostatic potential 3D map (a) and diene **2a** (b) optimized at the B3LYP/6-311++G(2d,2p) level of theory in acetone. Magenta circles indicate the bond critical points (BCP) in the compounds **1<sup>+</sup>** and **2** where the local descriptors are estimated.

suggest the latter atom as a more preferable site for nucleophilic attack (0.167 vs. 0.134). The latter  $f^+$  values for the rest cations are listed in Table S2 in the Supporting Information. It is worthwhile noting that the ring substituents slightly affect the ESP values on the allylic fragment, while the  $\text{CH}_3$  group in the cations **1<sup>+</sup>** causes a rather drastic effect. This also follows from the lower  $\omega$  indexes (Table 1).

Recently, we have found that a number of local Quantum Theory of Atoms in Molecules properties are convenient for the structure-activity description in benzidine and its singly and doubly oxidized forms.<sup>[49,50]</sup> Being calculated in the bond critical points (BCP), these can clarify the electron distribution and, consequently, the reactivity. Among these AIM quantities, we have used the electron density  $\rho(\mathbf{r})$ , its Laplacian  $\nabla^2\rho(\mathbf{r})$ , energy densities  $h_e(\mathbf{r})$ ,  $g(\mathbf{r})$ , and  $v(\mathbf{r})$ ,<sup>[51]</sup> bond ellipticity  $\varepsilon(\mathbf{r})$ ,<sup>[51]</sup> average local ionization energy  $\bar{I}(\mathbf{r})$ ,<sup>[52]</sup> localized orbital locator,<sup>[53]</sup> and electron localization function (ELF).<sup>[54]</sup> Figure 2(b) illustrates BCPs where the local descriptors are studied. The calculated data regarded to BCP1 are collected in Table 3, and the rest results (for BCP2 and BCP3) are included in the Supporting Information (Tables S3 and S4, respectively).

In contrast to the global molecular properties listed in Table 1, all the local descriptors, excluding several peculiar cases, do strongly correlate with the corresponding ( $\sigma_p$ ) constants. The average value of  $R^2$  is higher than 0.95 for all three BCPs. Actually, the correlation coefficients are even higher and often approach to 0.999, but such regression analysis requires more decimals to be accounted because the obtained values are very sensitive to rounding. The high  $R^2$  values suggest that every local molecular characteristic itself can serve as a reactivity descriptor, but the obtained absolute values should be compared with a proper reference structure. For this purpose, we have applied 2-butenyl cation (denoted as a *blank*). Thus, we can estimate how the whole arylsulfonyl group affects the pure 1,3-butadiene reactivity.

Surprisingly, the local descriptors suggest that the electron density is *donated* to the C(1)–C(2), C(2)–C(3), and C(3)–C(4) bonds compared with the blank (see the corresponding  $\rho(\mathbf{r})$  values in Tables 3, S3, and S4). Thus, one can conclude that the  $\text{SO}_2\text{Ar}$  group behaves as an *electron-donating substituent*. This also follows from the highest ESP values of the cation **1a<sup>+</sup>** and of the blank (the bold values in Fig. 2). As one can see in Fig. 2, the blank values of ESP are higher; this suggests that the  $\text{ArSO}_2$  group stabilizes the cation **1a<sup>+</sup>** (the highest and lowest values of ESP for the rest cations that are listed in Table S2 in the Supporting Information). Such interesting effect might be due to the cation stabilization by resonance, which can be illustrated in Scheme S1 (structures I–VIII) in the Supporting Information.

Additionally, the effect of hyperconjugation explains such behavior of the  $\text{ArSO}_2$  group. Indeed, the dihedral angle  $\varphi$  (Fig. S7) in the cation **1a<sup>+</sup>** is equal to  $99.1^\circ$ , and the  $l_{\text{C-S}} = 1.927 \text{ \AA}$ , that is noticeably higher than in the butene **1a** (1.840  $\text{ \AA}$ ). Moreover, the  $\rho(\mathbf{r})$  values at BCP corresponding to the C–S bond are equal to 0.1513 (**1a<sup>+</sup>**) and 0.1866 (**1a**), respectively. These structural and topological peculiarities prove the presence of an electron donation towards the allylic moiety and importance of hyperconjugation as a stabilizing factor (structures IX and X in Scheme S1). It is worthwhile noting that the increased  $\bar{I}(\mathbf{r})$  and ELF values in the cations **1<sup>+</sup>** can be ascribed to the inductive effect of the oxygen atoms counterbalancing to some extent hyperconjugation.

It is interesting that the electronic effect of the  $\text{CH}_3$  group in the cations **1<sup>+</sup>** results in decreasing  $\rho(\mathbf{r})$  values at BCP1 and BCP2, but its small increase at BCP3 (Tables 3, S3, and S4). This suggests an increased contribution of the resonance structure II (Scheme S1 in the Supporting Information). It is important that in the cation **1a<sup>+</sup>** the C–S bond elongation is less pronounced, possibly because the methyl group concurs to donate electron density via hyperconjugation:  $l_{\text{C-S}}$  are equal to 1.902  $\text{ \AA}$  (**1a<sup>+</sup>**) vs.

**Table 3.** The local molecular properties (in a. u.) of the cations  $1^+$  and  $1^{++}$  calculated at the  $r_1$  point (BCP1)

Entry	$ELF(r)$	$LOL(r)$	$\bar{l}(r)$	$\nabla^2\rho(r)$	$h_e(r)$	$v(r)$	$g(r)$	$\varepsilon(r)$	$\rho(r)$
Blank	0.9531	0.8184	0.6228	-0.7548	-0.2662	-0.3437	0.0775	0.0407	0.2825
$1a^+$	0.9563	0.8239	0.6468	-0.7734	-0.2714	-0.3494	0.0780	0.0573	0.2901
$1b^+$	0.9559	0.8231	0.6456	-0.7809	-0.2744	-0.3536	0.0792	0.0629	0.2918
$1c^+$	0.9555	0.8224	0.6436	-0.7866	-0.2768	-0.3570	0.0802	0.0676	0.2931
$1d^+$	0.9565	0.8243	0.6476	-0.7701	-0.2701	-0.3476	0.0775	0.0556	0.2894
$1e^+$	0.9565	0.8243	0.6476	-0.7690	-0.2697	-0.3471	0.0774	0.0552	0.2892
$1f^+$	0.9574	0.8258	0.6486	-0.7489	-0.2620	-0.3368	0.0748	0.0438	0.2851
$1g^+$	0.9573	0.8256	0.6503	-0.7566	-0.2647	-0.3417	0.0755	0.0471	0.2865
$1h^+$	0.9573	0.8257	0.6507	-0.7562	-0.2645	-0.3399	0.0754	0.0468	0.2864
$1i^+$	0.9568	0.8248	0.6489	-0.7636	-0.2675	-0.3441	0.0766	0.0515	0.2880
$1j^+$	0.9570	0.8251	0.6494	-0.7619	-0.2667	-0.3430	0.0763	0.0500	0.2876
$1a^+$	0.9582	0.8273	0.6350	-0.7171	-0.2509	-0.3224	0.0716	0.0428	0.2794
$1g^+$	0.9590	0.8288	0.6379	-0.7040	-0.2456	-0.3153	0.0696	0.0354	0.2765
$1h^+$	0.9590	0.8286	0.6383	-0.7047	-0.2459	-0.3156	0.0697	0.0355	0.2767
$R^2$	<b>0.9665</b>	<b>0.9602</b>	<b>0.9529</b>	<b>0.9675</b>	<b>0.9673</b>	<b>0.9651</b>	<b>0.9588</b>	<b>0.9483</b>	<b>0.9641</b>

The boldface style has been chosen to readily discriminate the  $R^2$  values from that of descriptors, which are often very similar.

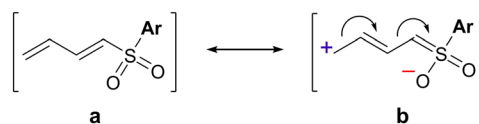
**Table 4.** The local molecular properties of the dienes  $2$  calculated at the  $r_1$  point (BCP1)

Entry	$ELF(r)$	$LOL(r)$	$\bar{l}(r)$	$\nabla^2\rho(r)$	$h_e(r)$	$v(r)$	$g(r)$	$\varepsilon(r)$	$\rho(r)$
Blank	0.9324	0.7879	0.5845	-0.9993	-0.3794	-0.5090	0.1296	0.3319	0.3425
$2a$	0.9299	0.7846	0.6237	-0.9742	-0.3739	-0.5043	0.1304	0.3179	0.3397
$2b$	0.9298	0.7845	0.6230	-0.9744	-0.3741	-0.5046	0.1305	0.3185	0.3398
$2c$	0.9298	0.7845	0.6223	-0.9744	-0.3741	-0.5047	0.1305	0.3191	0.3398
$2d$	0.9300	0.7847	0.6252	-0.9734	-0.3735	-0.5037	0.1302	0.3171	0.3396
$2e$	0.9300	0.7847	0.6252	-0.9735	-0.3735	-0.5037	0.1302	0.3169	0.3396
$2f$	0.9306	0.7855	0.6265	-0.9717	-0.3723	-0.5016	0.1293	0.3114	0.3392
$2g$	0.9302	0.7850	0.6278	-0.9725	-0.3730	-0.5028	0.1298	0.3153	0.3393
$2h$	0.9303	0.7851	0.6281	-0.9722	-0.3727	-0.5023	0.1296	0.3139	0.3392
$2i$	0.9301	0.7849	0.6261	-0.9731	-0.3733	-0.5032	0.1300	0.3157	0.3395
$2j$	0.9302	0.7850	0.6269	-0.9728	-0.3731	-0.5030	0.1299	0.3152	0.3394
$R^2$	<b>0.9895</b>	<b>0.9745</b>	<b>0.9957</b>	<b>0.9748</b>	<b>0.9803</b>	<b>0.9865</b>	<b>0.9649</b>	<b>0.9882</b>	<b>0.9595</b>

The boldface style has been chosen to readily discriminate the  $R^2$  values from that of descriptors, which are often very similar.

1.927 Å ( $1a^+$ ). Although the local descriptors in the cations  $1^+$  and  $1^{++}$  behave in a different manner compared with the blank, the global electrophilicity parameter takes into account all the substituents effects, which is seen in the correlation between the  $\omega$  values and the local descriptors.

Another aim of the present work is to study the peculiar reactivity of the dienes  $2$ . The optimized structures of the latter compounds together with the selected structural and infrared spectral parameters are presented in Fig. S8 in the Supporting Information. On one hand, the latter compounds hardly react in the Diels–Alder condensation (see the previous section). When reacting with aryl diazonium salts in the  $SO_2$  saturated medium, these compounds behave as isolated rather than conjugated dienes.<sup>[3–6]</sup> Thus, the carbon atoms C(3) and C(4) appear to be operating and crucial, not the C(1) and C(4) atoms. Similar to the consideration of the allylic cations, we have calculated the local molecular properties at the BCPs (Fig. 2) of the dienes  $2$  in order to rationalize their reactivity. The obtained data are listed in Tables 4, S5, and S6. In contrast to the cations  $1^+$ , the electron distribution in dienes  $2$  behaves in a slightly different manner.

**Scheme 6.** Resonance structures of the diene  $2a$ 

A small electron depletion is observed in BCP1 and BCP3 compared with the blank (1,3-butadiene). Meanwhile, the  $\rho(r)$  value at BCP2 is higher. This is in accord with the rise of the polar resonance structure contribution (Scheme 6, structure **b**).

It is worth noting that the ring substituent in the dienes  $2$  has almost no effect on the structural parameters (Fig. S8 in the Supporting Information). Such shifting of the electron density towards the  $ArSO_2$  group (Scheme 6) should partly break the conjugated system. Among the great variety of methods for estimating the  $\pi$ -electron conjugation, we have used two-centered delocalization index  $\delta$  (2c-DI)<sup>[55–57]</sup> and localization index  $\lambda$  (LI)<sup>[55]</sup> as the most reliable descriptors. As one can see in Table 5, the three key descriptors, namely, 2c-DI, LI, and  $L_{AB}$  do exhaustively suggest a partial breaking of the conjugated system in the

**Table 5.** The two-centered delocalization (2c-DI) and localization (LI) indexes, Laplacian bond orders ( $L_{AB}$ ), and frontier molecular orbital energies of the dienes **2**

Entry	2c-DI ( $\delta$ )			LI ( $\lambda$ )				$L_{AB}$			$E_{HOMO}^a$ eV	$E_{LUMO}^a$ eV
	C1-C2	C2-C3	C3-C4	C1	C2	C3	C4	C1-C2	C2-C3	C3-C4		
Blank	1.8741	1.2145	1.8741	4.374	4.106	4.106	4.374	1.9157	1.3180	1.9157	-6.31	-0.69
<b>2a</b>	1.6903	1.2082	1.8534	4.005	4.028	4.105	4.340	1.8128	1.3149	1.9155	-6.84	-1.79
<b>2b</b>	1.6913	1.2081	1.8539	4.004	4.029	4.105	4.340	1.8140	1.3109	1.9158	-6.75	-1.76
<b>2c</b>	1.6921	1.2080	1.8544	4.003	4.030	4.105	4.341	1.8130	1.3131	1.9153	-6.42	-1.70
<b>2d</b>	1.6877	1.2086	1.8521	4.005	4.026	4.105	4.338	1.8087	1.3153	1.9141	-6.85	-1.88
<b>2e</b>	1.6875	1.2085	1.8520	4.005	4.026	4.105	4.338	1.8077	1.3142	1.9117	-6.82	-1.89
<b>2f</b>	1.6770	1.2088	1.8493	4.007	4.020	4.105	4.334	1.8028	1.3170	1.9112	-6.98	-2.85
<b>2g</b>	1.6842	1.2093	1.8504	4.008	4.024	4.105	4.336	1.8097	1.3169	1.9160	-6.99	-2.84
<b>2h</b>	1.6818	1.2097	1.8493	4.008	4.022	4.105	4.334	1.8054	1.3148	1.9125	-7.00	-2.97
<b>2i</b>	1.6856	1.2089	1.8512	4.006	4.024	4.105	4.337	1.8077	1.3132	1.9123	-6.93	-2.20
<b>2j</b>	1.6842	1.2091	1.8504	4.006	4.023	4.105	4.336	1.8056	1.3160	1.9110	-6.96	-2.11
<b>R<sup>2</sup></b>	<b>0.9927</b>	<b>0.9506</b>	<b>0.9941</b>	<b>0.8979</b>	<b>0.9958</b>	—	<b>0.9701</b>	<b>0.9013</b>	<b>0.3569</b>	<b>0.6848</b>	<b>0.7249</b>	<b>0.7293</b>

<sup>a</sup>Calculated using the DFT(B3LYP)/6-31G(d) method in acetone.

The boldface style has been chosen to readily discriminate the R2 values from that of descriptors, which are often very similar.

**Table 6.** Radical ( $f^0$ ), electrophilic ( $f^+$ ), and nucleophilic ( $f^-$ ) Fukui functions condensed to the diene carbon atoms in the dienes **2**

Entry	$f_A^+$				$f_A^0$				$f_A^-$			
	C(1)	C(2)	C(3)	C(4)	C(1)	C(2)	C(3)	C(4)	C(1)	C(2)	C(3)	C(4)
<b>2a</b>	0.091	0.102	0.064	0.135	0.098	0.086	0.078	0.141	0.105	0.070	0.091	0.146
<b>2b</b>	0.095	0.104	0.067	0.140	0.090	0.083	0.069	0.130	0.084	0.062	0.072	0.120
<b>2c</b>	0.101	0.106	0.071	0.146	0.068	0.072	0.051	0.102	0.035	0.037	0.030	0.058
<b>2d</b>	0.085	0.097	0.060	0.127	0.087	0.079	0.068	0.126	0.089	0.062	0.077	0.126
<b>2e</b>	0.086	0.099	0.060	0.127	0.081	0.076	0.062	0.117	0.075	0.054	0.064	0.107
<b>2f</b>	0.006	0.019	0.007	0.020	0.065	0.046	0.058	0.095	0.124	0.074	0.110	0.169
<b>2g</b>	0.002	0.008	0.003	0.010	0.064	0.042	0.058	0.091	0.126	0.076	0.112	0.173
<b>2h</b>	0.007	0.018	0.007	0.020	0.067	0.046	0.060	0.096	0.126	0.074	0.113	0.173
<b>2i</b>	0.038	0.055	0.028	0.065	0.077	0.063	0.065	0.113	0.117	0.072	0.103	0.161
<b>2j</b>	0.042	0.060	0.030	0.070	0.077	0.063	0.068	0.114	0.113	0.066	0.105	0.158
Blank	0.194	0.112	—	—	0.198	0.115	—	—	0.202	0.118	—	—

dienes **2**. When compared with the blank, the aforementioned parameters in the bond C(1)–C(2) are sharply decreased. The farther the bond is distant from the  $ArSO_2$  group, the more the calculated values approach to those of the blank. The high correlations of the 2c-DI, LI, and  $L_{AB}$  values with the corresponding Hammett ( $\sigma_p$ ) constants indicate that the influence of the  $SO_2Ar$  group does proceed through the  $\pi$  system. The electron density depletion from the diene moiety in compounds **2** decreases significantly their reactivity towards the Diels–Alder condensation (Scheme 2). A simple descriptor – the highest occupied molecular orbital energy value ( $E_{HOMO}$ ) – has been used to elucidate the relative ability of the dienes **2** in the latter reaction. When compared with the blank, all the  $E_{HOMO}$  values are lower (Table 5); this means that the more energy is needed for breaking the conjugated system. Indeed, the dienes **2** require melting at rather high temperatures to undergo the Diels–Alder reaction (Experimental Section). Thus, the obtained theoretical results completely confirm the experimental findings.

Finally, we have calculated the Fukui functions condensed to the carbon atoms in the diene moiety; the results are listed in Table 6. The first conclusion, which follows from the lower  $f^-$ ,

$f^0$ ,  $f^+$  values of the dienes **2** compared with bare 1,3-butadiene (Table 6), is that these are less reactive towards the addition reactions. Secondly, despite the electron withdrawing nature of the  $ArSO_2$  group, the electrophilic addition to the dienes **2** is a more preferable reaction pathway, than the radical and, especially, nucleophilic attack. Moreover, the highest values of the Fukui functions are characteristic to the C(4) atoms; thus, taking into account the partly broken conjugated system, we can confirm computationally that the addition to the dienes **2** does proceed via the C(4) and C(3) carbon atoms.<sup>[3–6]</sup>

## CONCLUSIONS

In the present work, we have studied reactivity of 13 various ring-substituted 1-(arylsulfonyl)-2-R-4-chloro-2-butenes towards both nucleophilic substitution and elimination reactions. The experiments have revealed that these dienes easily undergo  $S_N$  reactions with amines (diethylamine, morpholine, and diethanolamine), KOH, and  $Na_2S$ . The high reactivity has been rationalized in terms of an effective resonance stabilization of

the intermediate allylic cations, which has been determined from the ESP values and the local reactivity descriptors, namely,  $\rho(\mathbf{r})$ ,  $\bar{I}(\mathbf{r})$ , and  $ELF$ . The obtained reaction yields correlate with the theoretical log  $k$  values computed by means of the Mayr–Patz equation, which has included the global electrophilicity index ( $\omega$ ) and the adiabatic nucleophilicity index ( $N_{ad}$ ). The good linear correlations ( $R^2 \sim 0.97$ ) of the reactivity parameters of the allylic cations with the corresponding Hammett  $\sigma_p$  constants of the ring substituents have indicated that their influence predominantly proceeds via the  $\pi$  system.

The elimination of hydrogen chloride from 1-(arylsulfonyl)-2-*R*-4-chloro-2-butenes has yielded the corresponding 1-arylsulfonyl 1,3-dienes. These compounds were characterized experimentally as poor dienes in the Diels–Alder condensation. The calculations have revealed that these have lower HOMO energies compared with bare 1,3-butadiene that explains their general inactivity. The computed values of the 2c-DI and LI of the studied dienes have allowed us to elucidate why these compounds behave as isolated rather than conjugated dienes in addition reactions.<sup>[3–5]</sup> The mechanism of the latter reactions with aryl diazonium salts in the  $SO_2$  saturated medium, however, is still not yet completely clear.

Obushak *et al.*<sup>[58–61]</sup> put forward the most exhaustive proposal, which included an intermediate formation of the radical cation of the reaction substrate (diene). At the same time, we have recently found that the transition state of addition reaction to the double C=C bond of  $\pi$ -nucleophiles has a multireference nature with a high contribution of the triplet  $^3\pi\pi^*$  state of the latter.<sup>[35]</sup> Consequently, the triplet states of  $\pi$ -nucleophiles should be considered when estimating the activation barrier of this reaction.<sup>[35,62–67]</sup> Moreover, our recent results suggest that the aforementioned  $^3\pi\pi^*$  states can be achieved under the “dark” conditions by the action of catalyst (copper fine particles).<sup>[68]</sup> Therefore, the complete understanding of the dienes **2** reactivity still remains to be a puzzle for both experimentalists and theoreticians.

## EXPERIMENTAL SECTION

### General

The  $^1H$  NMR spectra were recorded using Varian VXR-300 and Varian Gemini-400 spectrophotometers in  $CDCl_3$ ,  $DMSO-d_6$ , or  $Me_2CO-d_6$  solvents. Reaction solvents were dried and distilled under nitrogen using standard procedures. All commercially available reactants were purchased from Aldrich, ALSI Ltd. Kiev, Ukraine and used without further purification. 1-(Arylsulfonyl)-4-chloro-2-butenes were prepared according to our previously developed protocol<sup>[69]</sup> and were recrystallized before use.

### General procedure for the synthesis of 1-arylsulfonyl 1,3-butadienes (2a–2j)

To a solution of the corresponding 1-(arylsulfonyl)-4-chloro-2-butene (0.05 mol) in 130 mL of benzene, a solution of 6.9 mL of triethylamine (0.05 mol) in 20 mL of benzene was added dropwise. The reaction mixture was refluxed on a water bath at 70–80 °C for 3 h. After cooling the reaction mixture, a precipitate of triethylamine hydrochloride was separated, then benzene was distilled off under reduced pressure, and the residue was recrystallized. Solvents for recrystallization of the compounds **2a–2c**, **2d–2g**, **2h–2i**, and **2j** were the following: hexane, ethanol–water 2/1 mixture, ethanol–water 1/2 mixture, and ethanol–water 1/1 mixture, respectively.

### Compound 2a

Yield 73% (based on triethylamine), oily compound (crystallizes upon cooling in ice water). Anal. Calcd for  $C_{10}H_{10}O_2S$ : S, 16.50. Found: S, 16.41; Calcd: C, 61.83. Found: C, 62.05; Calcd: H, 5.19. Found: H, 5.27.

### Compound 2b

Yield 87% (based on triethylamine), oily compound (crystallizes upon cooling in ice water). Anal. Calcd for  $C_{11}H_{12}O_2S$ : S, 15.39. Found: S, 15.22; Calcd: C, 63.43. Found: C, 63.68; Calcd: H, 5.81. Found: H, 5.96.

### Compound 2c

Yield 83% (based on triethylamine), oily compound (crystallizes upon cooling in ice water). Anal. Calcd for  $C_{11}H_{12}O_3S$ : S, 14.29. Found: S, 14.16; Calcd: C, 58.91. Found: C, 58.98; Calcd: H, 5.39. Found: H, 5.60.

### Compound 2d

Yield 53% (based on triethylamine), oily compound (crystallizes upon cooling in ice water). Anal. Calcd for  $C_{10}H_9ClO_2S$ : Cl, 15.50. Found: Cl, 15.20; Calcd: S, 14.02. Found: S, 14.24; Calcd: C, 52.52. Found: C, 52.83; Calcd: H, 3.97. Found: H, 4.08.

### Compound 2e

Yield 69%, mp: 44–45 °C. Anal. Calcd for  $C_{10}H_9BrO_2S$ : Br, 29.25. Found: Br, 28.84; Calcd: S, 11.74. Found: S, 12.05; Calcd: C, 43.97. Found: C, 44.21; Calcd: H, 3.32. Found: H, 3.40.

### Compound 2f

Yield 62%, mp: 79–80 °C.  $^1H$  NMR (600 MHz,  $CDCl_3$ )  $\delta$ : 5.67–5.70 (d,  $J = 9$  Hz, 1H,  $CH_2$ ), 5.76–5.82 (d,  $J = 17.1$  Hz, 1H, CH), 5.42–6.54 (m, 1H, CH), 6.86–6.91 (d,  $J = 15$  Hz, 1H, CH), 7.29–7.32 (m, 1H, CH), 7.77–7.83 (m, 3H, *o*- $O_2NC_6H_4$ ), 8.16–8.19 (dd, 1H, *o*- $O_2NC_6H_4$ ); The  $^1H$  NMR spectrum of the diene **2j**:  $^1H$  NMR (600 MHz,  $CDCl_3$ )  $\delta$ : 4.92 (s, 2H,  $NH_2$ ), 5.67–5.70 (d,  $J = 9.0$  Hz, 1H, CH), 5.78–5.82 (d,  $J = 17.0$  Hz, 1H, CH), 6.37–6.40–6.44 (m, 2H,  $CH_2$ ), 7.30–7.32–7.33–7.35 (dd,  $J_1 = 11.0$ ,  $J_2 = 11.5$  Hz, 1H, CH), 8.04–8.06 (d,  $J = 8.0$  Hz, 2H,  $C_6H_4$ ), 8.09–8.11 (d,  $J = 7.5$  Hz, 2H, *p*- $H_2NSO_2C_6H_4$ ); Anal. Calcd for  $C_{10}H_9NO_4S$ : N, 5.55. Found: N, 5.70; Calcd: S, 13.40. Found: S, 13.27; Calcd: C, 50.20. Found: C, 50.29; Calcd: H, 3.79. Found: H, 3.93.

### Compound 2g

Yield 76%, mp: 61–62 °C. Anal. Calcd for  $C_{10}H_9NO_4S$ : N, 5.55. Found: N, 5.76; Calcd: S, 13.40. Found: S, 13.65; Calcd: C, 50.20. Found: C, 50.41; Calcd: H, 3.79. Found: H, 3.95.

### Compound 2h

Yield 95%, mp: 102–103 °C. Anal. Calcd for  $C_{10}H_9NO_4S$ : N, 5.55. Found: N, 5.76; Calcd: S, 13.40. Found: S, 13.60; Calcd: C, 50.20. Found: C, 50.38; Calcd: H, 3.79. Found: H, 3.87.

### Compound 2i

Yield 92%, mp: 174–175 °C. Anal. Calcd for  $C_{11}H_{10}O_4S$ : S, 13.45. Found: S, 13.20; Calcd: C, 55.45. Found: C, 55.20; Calcd: H, 4.23. Found: H, 4.06.

### Compound 2j

Yield 48%, mp: 184–185 °C. Anal. Calcd for  $C_{10}H_{11}NO_4S_2$ : N, 5.12. Found: N, 5.02; Calcd: S, 23.46. Found: S, 23.73; Calcd: C, 43.94. Found: C, 44.05; Calcd: H, 4.05. Found: H, 4.29.

**General procedure for the synthesis of anhydrides of 1-(arylsulfonyl)-1,4,5,6-tetrahydrophthalic acid (3g–3j)**

The corresponding 1-arylsulfonyl 1,3-butadiene (0.01 mol) was mixed with 1 g (0.01 mol) of freshly sublimed maleic anhydride, and then the mixture was alloyed for 6 h. After cooling, the solid melt was separated and recrystallized. The compound **3g** was recrystallized from benzene and the compounds **3h–3j** form glacial acetic acid.

**Compound 3g**

Yield 15%, mp: 133–134 °C.  $^1\text{H NMR}$  (600 MHz,  $\text{CDCl}_3$ )  $\delta$ : 2.56 (m, 2H,  $\text{CH}_2$ ), 3.84 (m, 2H in  $\text{CHCO}$ ), 5.03 (t, 1H, CH), 5.67 (t, 1H, CH), 6.29 (m, 1H in  $\text{CHSO}_2$ ), 7.94–7.95–7.97 (t,  $J_1 = 7.5$ ,  $J_2 = 8.0$  Hz, 1H,  $m\text{-O}_2\text{NC}_6\text{H}_4$ ), 8.26–8.28 (d, 1H,  $J = 8.0$  Hz,  $m\text{-O}_2\text{NC}_6\text{H}_4$ ), 8.57 (d, 1H,  $m\text{-O}_2\text{NC}_6\text{H}_4$ ), 8.59 (s, 1H,  $m\text{-O}_2\text{NC}_6\text{H}_4$ ). The  $^1\text{H NMR}$  spectrum of the adduct **3h**:  $^1\text{H NMR}$  (600 MHz,  $\text{CDCl}_3$ )  $\delta$ : 2.49–2.55 (m, 1H, CH), 2.59 (m, 1H, CH), 3.85 (m, 2H,  $\text{CH}_2$ ), 4.98–4.99–5.01 (t, 1H, CH), 5.62 (t, 1H, CH), 6.28 (m, 1H, CH), 8.12–8.13 (d,  $J = 9.0$  Hz, 2H,  $p\text{-O}_2\text{NC}_6\text{H}_4$ ), 8.44–8.46 (d,  $J = 9.0$  Hz, 2H,  $p\text{-O}_2\text{NC}_6\text{H}_4$ ); Anal. Calcd for  $\text{C}_{14}\text{H}_{11}\text{NO}_7\text{S}$ : N, 4.15. Found: N, 4.12; Calcd: S, 9.50. Found: S, 9.66; Calcd: C, 49.85. Found: C, 50.07; Calcd: H, 3.29. Found: H, 3.45.

**Compound 3h**

Yield 17%, mp: 203–204 °C. Anal. Calcd for  $\text{C}_{14}\text{H}_{11}\text{NO}_7\text{S}$ : N, 4.15. Found: N, 3.92; Calcd: S, 9.50. Found: S, 9.70; Calcd: C, 49.85. Found: C, 50.10; Calcd: H, 3.29. Found: H, 3.47.

**Compound 3i**

Yield 11%, mp: 257–280 °C (decomposition). Anal. Calcd for  $\text{C}_{15}\text{H}_{12}\text{O}_7\text{S}$ : S, 9.53. Found: S, 9.36; Calcd: C, 53.57. Found: C, 53.71; Calcd: H, 3.59. Found: H, 3.68.

**Compound 3j**

Yield 19%, mp: 200–250 °C (decomposition). Anal. Calcd for  $\text{C}_{14}\text{H}_{13}\text{NO}_7\text{S}_2$ : N, 3.77. Found: N, 3.62; Calcd: S, 17.27. Found: S, 17.44; Calcd: C, 45.28. Found: C, 45.50; Calcd: H, 3.53. Found: H, 3.77.

**General procedure for the synthesis of 1-(arylsulfonyl)-4-N,N-dialkylamino-2-butenes (4–6)**

To a solution of the corresponding 1-(arylsulfonyl)-2-R-4-chloro-2-butene (0.02 mol) in 20 mL of acetone a solution of the corresponding secondary amine (0.02 mol) in 5 mL of acetone was added dropwise. The reaction mixture was refluxed on a water bath at 70–80 °C for 1 h. After cooling, the reaction mixture was poured into 50 mL of water, and then sodium carbonate was added until a slightly alkali reaction. The formed precipitate was separated and recrystallized. Solvents for recrystallization of the compounds were the following: ethanol–water 2/1 mixture (**4e**), ethanol–water 1/2 mixture (**4j**), ethanol–water 1/1 mixture (**4g** and **6j**), and neat water (**5j**, **5a**, and **5h**).

**Compound 4e**

Yield 34%, mp: 198–199 °C. Anal. Calcd for  $\text{C}_{14}\text{H}_{20}\text{BrNO}_2\text{S}$ : N, 3.97. Found: N, 4.04; Calcd: Br, 23.07. Found: Br, 22.90; Calcd: S, 9.26. Found: S, 9.43; Calcd: C, 48.56. Found: C, 48.72; Calcd: H, 5.82. Found: H, 5.95.

**Compound 4j**

Yield 31%, mp: 219–220 °C. Anal. Calcd for  $\text{C}_{14}\text{H}_{22}\text{N}_2\text{O}_4\text{S}_2$ : N, 7.94. Found: N, 8.08; Calcd: S, 18.51. Found: S, 18.70; Calcd: C, 48.53. Found: C, 48.67; Calcd: H, 6.40. Found: H, 6.45.

**Compound 4g**

Yield 37%, mp: 163–164 °C. Anal. Calcd for  $\text{C}_{15}\text{H}_{22}\text{N}_2\text{O}_4\text{S}$ : N, 8.56. Found: N, 8.58; Calcd: S, 9.82. Found: S, 10.03; Calcd: C, 55.19. Found: C, 55.27; Calcd: H, 6.72. Found: H, 6.83.

**Compound 5j**

Yield 32%, mp: 168–169 °C. Anal. Calcd for  $\text{C}_{14}\text{H}_{20}\text{N}_2\text{O}_5\text{S}_2$ : N, 7.63. Found: N, 7.77; Calcd: S, 17.79. Found: S, 17.60; Calcd: C, 46.65. Found: C, 46.44; Calcd: H, 5.59. Found: H, 5.49.

**Compound 5a**

Yield 53%, mp: 98–99 °C.  $^1\text{H NMR}$  (600 MHz,  $\text{CDCl}_3$ )  $\delta$ : 1.85 (s, 3H,  $\text{CH}_3$ ), 2.29 (t, 4H,  $\text{CH}_2$ ), 2.93–2.94 (d,  $J = 6.5$  Hz, 2H,  $\text{CH}_2$ ), 3.66 (t, 4H,  $\text{CH}_2$ ), 3.81 (s, 2H,  $\text{CH}_2$ ), 5.25 (t, 1H, CH), 7.55–7.57–7.58 (t,  $J_1 = 7.0$ ,  $J_2 = 7.5$  Hz, 2H,  $\text{C}_6\text{H}_5$ ), 7.64–7.66–7.67 (t, 1H,  $\text{C}_6\text{H}_5$ ), 7.87–7.89 (d,  $J = 8.0$  Hz, 2H,  $\text{C}_6\text{H}_5$ ); Anal. Calcd for  $\text{C}_{15}\text{H}_{21}\text{NO}_3\text{S}$ : N, 5.00. Found: N, 4.74; Calcd: S, 10.85. Found: S, 10.89; Calcd: C, 60.99. Found: C, 61.10; Calcd: H, 7.16. Found: H, 7.28.

**Compound 5h**

Yield 41%, mp: 137–138 °C.  $^1\text{H NMR}$  (600 MHz,  $\text{CDCl}_3$ )  $\delta$ : 1.71 (s, 3H,  $\text{CH}_3$ ), 2.07 (s, 4H,  $\text{CH}_2$ ), 2.78–2.79 (d,  $J = 7.0$  Hz, 2H,  $\text{CH}_2$ ), 3.34–3.50 (m, 4H,  $\text{CH}_2$ ), 4.23 (s, 2H,  $\text{CH}_2$ ), 5.19 (t, 1H, CH), 8.12–8.14 (d,  $J = 9.5$  Hz, 2H,  $p\text{-O}_2\text{NC}_6\text{H}_4$ ), 8.42–8.44 (d,  $J = 8.5$  Hz, 2H,  $p\text{-O}_2\text{NC}_6\text{H}_4$ ); Anal. Calcd for  $\text{C}_{15}\text{H}_{20}\text{N}_2\text{O}_5\text{S}$ : N, 8.44. Found: N, 8.23; Calcd: S, 9.42. Found: S, 9.39; Calcd: C, 52.93. Found: C, 53.12; Calcd: H, 5.92. Found: H, 5.98.

**Compound 6j**

Yield 31%, mp: 191–192 °C. Anal. Calcd for  $\text{C}_{14}\text{H}_{22}\text{N}_2\text{O}_6\text{S}_2$ : N, 7.35. Found: N, 7.40; Calcd: S, 8.47. Found: S, 8.28; Calcd: C, 44.43. Found: C, 44.80; Calcd: H, 5.86. Found: H, 5.99.

**General procedure for the synthesis of 1-(arylsulfonyl)-2-R-2-buten-4-ols (7)**

To a solution of the corresponding 4-substituted 1-(arylsulfonyl)-2-butene (0.02 mol) in 30 mL of acetone, a solution of 1.12 g (0.02 mol) of potassium hydroxide in 10 mL of water was added dropwise. The reaction mixture was heated until dissolving and left at room temperature for 1 h. Then it was poured in 100 mL of water. The formed solid phase was separated and recrystallized. The compounds **7g** and **7h** were recrystallized from a mixture of acetic acid–water 1/2, the compound **7h** from a mixture of ethanol–water 1/1, and the compound **7j** from a mixture of ethanol–water 1/2.

**Compound 7g**

Yield 59%, mp: 71–72 °C. Anal. Calcd for  $\text{C}_{10}\text{H}_{11}\text{NO}_5\text{S}$ : N, 5.44. Found: N, 5.18; Calcd: S, 12.46. Found: S, 12.22; Calcd: C, 46.69. Found: C, 46.74; Calcd: H, 4.31. Found: H, 4.52.

**Compound 7h**

Yield 61%, mp: 109–110 °C. Anal. Calcd for  $\text{C}_{10}\text{H}_{11}\text{NO}_5\text{S}$ : N, 5.44. Found: N, 5.24; Calcd: S, 12.46. Found: S, 12.20; Calcd: C, 46.69. Found: C, 46.77; Calcd: H, 4.31. Found: H, 4.49.

**Compound 7j**

Yield 37%, mp: 165–166 °C. Anal. Calcd for  $\text{C}_{10}\text{H}_{13}\text{NO}_5\text{S}_2$ : N, 4.80. Found: N, 4.87; Calcd: S, 22.01. Found: S, 22.20; Calcd: C, 41.22. Found: C, 41.48; Calcd: H, 4.50. Found: H, 4.59.

### Compound 7'h

Yield 43%, mp: 89–90 °C. Anal. Calcd for C<sub>11</sub>H<sub>13</sub>NO<sub>5</sub>S: N, 5.16. Found: N, 5.22; Calcd: S, 11.82. Found: S, 11.60; Calcd: C, 48.70. Found: C, 48.68; Calcd: H, 4.83. Found: H, 4.73.

### General procedure for the synthesis of bis[4-(arylsulfonyl)-3-R-but-2-enyl]sulfides (8)

To a solution of the corresponding 1-(arylsulfonyl)-2-R-4-chloro-2-butene (0.02 mol) in 40 mL of acetone, a solution of 2.4 g (0.01 mol) of Na<sub>2</sub>S 9H<sub>2</sub>O in 15 mL of water was added dropwise. The reaction mixture was left at room temperature for 1 h and then poured in 100 mL of water. The formed solid phase was separated and recrystallized. The compounds **8g**, **8h**, **8j**, and **8'h** were recrystallized from glacial acetic acid and the compound **8i** from a mixture of acetic acid–water 1/2.

### Compound 8g

Yield 66%, mp: 158–159 °C. <sup>1</sup>H NMR (600 MHz, CDCl<sub>3</sub>) δ 2.86–2.87 (d, 4H, CH<sub>2</sub>), 4.26–4.27 (d, 4H, CH<sub>2</sub>), 5.36 (m, 2H, CH), 5.51 (m, 2H, CH), 7.93–7.95–7.96 (t, J<sub>1</sub> = 8.0, J<sub>2</sub> = 8.0 Hz, 2H, m-O<sub>2</sub>NC<sub>6</sub>H<sub>4</sub>), 8.26–8.28 (d, J = 6.5 Hz, 2H, m-O<sub>2</sub>NC<sub>6</sub>H<sub>4</sub>), 8.53–8.55–8.57 (t, J<sub>1</sub> = 9.5, J<sub>2</sub> = 9.5 Hz, 4H, m-O<sub>2</sub>NC<sub>6</sub>H<sub>4</sub>); Anal. Calcd for C<sub>20</sub>H<sub>20</sub>N<sub>2</sub>O<sub>8</sub>S<sub>3</sub>: N, 5.46. Found: N, 5.39; Calcd: S, 18.77. Found: S, 18.50; Calcd: C, 46.86. Found: C, 46.57; Calcd: H, 3.93. Found: H, 3.84.

### Compound 8h

Yield 65%, mp: 191–192 °C. <sup>1</sup>H NMR (600 MHz, CDCl<sub>3</sub>) δ 2.87–2.88 (d, 4H, CH<sub>2</sub>), 4.25–4.26 (d, 4H, CH<sub>2</sub>), 5.34 (m, 2H, CH), 5.53 (m, 2H, CH), 8.11–8.12 (d, J = 8.5 Hz, 4H, p-O<sub>2</sub>NC<sub>6</sub>H<sub>4</sub>), 8.43–8.45 (d, J = 9.0 Hz, 4H, p-O<sub>2</sub>NC<sub>6</sub>H<sub>4</sub>); Anal. Calcd for C<sub>20</sub>H<sub>20</sub>N<sub>2</sub>O<sub>8</sub>S<sub>3</sub>: N, 5.46. Found: N, 5.33; Calcd: S, 18.77. Found: S, 18.49; Calcd: C, 46.86. Found: C, 46.51; Calcd: H, 3.93. Found: H, 3.72.

### Compound 8i

Yield 70%, mp: 217–218 °C. Anal. Calcd for C<sub>22</sub>H<sub>22</sub>O<sub>8</sub>S<sub>3</sub>: S, 18.84. Found: S, 18.95; Calcd: S, 18.84. Found: S, 19.01; Calcd: C, 51.75. Found: C, 51.90; Calcd: H, 4.34. Found: H, 4.47.

### Compound 8j

Yield 40%, mp: 245–246 °C. Anal. Calcd for C<sub>20</sub>H<sub>24</sub>N<sub>2</sub>O<sub>8</sub>S<sub>5</sub>: N, 4.82. Found: N, 4.75; Calcd: S, 27.61. Found: S, 27.39; Calcd: C, 41.36. Found: C, 41.10; Calcd: H, 4.16. Found: H, 3.93.

### Compound 8'h

Yield 54%, mp: 175–176 °C. Anal. Calcd for C<sub>22</sub>H<sub>24</sub>N<sub>2</sub>O<sub>8</sub>S<sub>3</sub>: N, 5.18. Found: N, 5.30; Calcd: S, 17.79. Found: S, 17.64; Calcd: C, 48.87. Found: C, 48.66; Calcd: H, 4.47. Found: H, 4.29.

### Computational details

All the geometry optimizations and spectra calculations have been performed using Gaussian09 program package.<sup>[70]</sup> We have selected DFT<sup>[71]</sup>/B3LYP<sup>[72,73]</sup> method with Pople's split-valence almost triple- $\zeta$  in the valence shell basis set (6–311 G) and addition of both polarization (2d,2p) and diffuse (++) functions.<sup>[74,75]</sup> Thus, the complete notation of the method used is as the following, DFT(B3LYP)/6-311++G(2d,2p). In order to obtain reliable values of the IE and EA energies, we have used the aforementioned level of theory with adding both polarization and diffuse functions.<sup>[34]</sup> Despite the studied systems are either neutral or cationic species, such basis set extension is required.<sup>[34]</sup> To justify the obtained geometries as the minima (number of imaginary frequencies (NIMAG) = 0) or the first-order saddle points (NIMAG = 1), the vibrational frequency analysis was subsequently performed.

To describe the studied interactions as a realistic feature of condensed phase, the polarizable continuum model simulations have been included.<sup>[76]</sup> Acetone was chosen as a model medium because it is used in the studied synthesis. To define cavities the universal force field radii were used.<sup>[76]</sup> The overlap index and a minimum radius of the spheres were specified as 0.8 and 0.5 Å, respectively. The DFT calculations of the closed-shell species were performed using the spin-restricted Kohn–Sham formalism, while the open-shell species were calculated in terms of the spin-unrestricted Kohn–Sham approach.

The Quantum Theory of Atoms in Molecules properties<sup>[51]</sup> have been calculated using the AIMQB program within the AIMStudio suite using the Proaim basin integration method.<sup>[77]</sup> A part of post-SCF analyses were performed with a recently developed Multiwfn program package.<sup>[78]</sup> The condensed Fukui functions and the dual descriptor values have been computed using the atomic charges determined by the Hirshfeld population analysis.<sup>[79]</sup> This part of calculations was treated using the DFT(BLYP)/TNP method implemented in Materials Studio 5.5 suite of programs.<sup>[80]</sup> Wherein, the polar medium simulation was performed using a conductor-like screening model.<sup>[81]</sup>

### Acknowledgements

This work was supported by the Ministry of Education and Science of Ukraine, Research Fund (Grant No. 0113U001694). We thank Professor Hans Ågren (KTH, Stockholm) for the PDC supercomputer use. The computations were performed on resources provided by the Swedish National Infrastructure for Computing (SNIC) at the Parallel Computer Center (PDC) through the project "Multiphysics Modeling of Molecular Materials," SNIC 020/11-23.

### REFERENCES

- [1] S. W. Lee, H. B. Lee, B. C. Kim, K. Sadaiah, K. Lee, H. Shin, *Bull. Kor Chem. Soc.* **2013**, *34*, 1257–1259.
- [2] F.-S. Mu, M. Luo, Y.-J. Fu, X. Zhang, P. Yu, Y.-G. Zu, *Molecules*. **2011**, *16*, 4097–4103.
- [3] V. V. Smalius, V. M. Naidan, *Russ. J. Gen. Chem.* **2011**, *81*, 566–568.
- [4] V. V. Smalius, V. M. Naidan, *Russ. J. Gen. Chem.* **2007**, *77*, 586–588.
- [5] V. V. Smalius, V. M. Naidan, *Russ. J. Gen. Chem.* **2006**, *76*, 1295–1298.
- [6] D. Díez, S. G. Sanfeliciano, J. Peña, M. Fe Flores, P. García, N. M. Garrido, I. S. Marcos, A. J. White, P. Basabe, J. G. Urones, *Arkivoc.* **2011**, *3*, 6–19.
- [7] D. Díez, M. Templo Benítez, I. S. Marcos, N. M. Garrido, P. Basabe, J. G. Urones, *Molecules*. **2004**, *9*, 323–329.
- [8] D. Díez, M. Templo Benítez, I. S. Marcos, N. M. Garrido, P. Basabe, J. G. Urones, *Synlett*. **2001**, 655–657.
- [9] J. G. Urones, I. S. Marcos, N. M. Garrido, P. Basabe, A. J. Bastida, S. J. San Feliciano, D. Díez, J. M. Goodman, *Synlett*. **1998**, 1361–1363.
- [10] J. G. Urones, I. S. Marcos, N. M. Garrido, P. Basabe, S. J. San Feliciano, R. Coca, D. Díez, *Synlett*. **1998**, 1364–1365.
- [11] J.-H. Min, J.-S. Lee, J.-D. Yang, S. Koo, *J. Org. Chem.* **2003**, *68*, 7925–7927.
- [12] V. M. Naidan, V. V. Smalius, *Russ. J. Gen. Chem.* **2005**, *75*, 1771–1773.
- [13] V. M. Naidan, V. V. Smalius, *Russ. J. Gen. Chem.* **2005**, *75*, 580–582.
- [14] C. S. Hampton, M. Harmata, *Org. Lett.* **2014**, *16*, 1256–1259.
- [15] J.-E. Bäckvall, R. Chinchilla, C. Nájera, M. Yus, *Chem. Rev.* **1998**, *98*, 2291–2312 (and references therein).
- [16] A. C. Flick, A. Padwa, *J. Sulfur Chem.* **2013**, *34*, 1–16 (and references therein).
- [17] A. C. Flick, A. Padwa, *J. Sulfur Chem.* **2013**, *34*, 7–16 (and references therein).
- [18] E. L. Luzina, A. V. Popov, *J. Fluor. Chem.* **2013**, *148*, 41–48.
- [19] M. Ghosh, S. Dutta, U. Sanyal, *Neoplasma*. **1999**, *46*, 242–245.
- [20] A. Yacovan, R. Ozeri, T. Kehat, S. Mirilashvili, D. Sherman, A. Aizikovitch, A. Shitrit, E. Ben-Zeev, N. Schutz, O. Bohana-Kashtan, A. Konson, V. Behar, O. M. Becker, *Bioorg. Med. Chem. Lett.* **2012**, *22*, 6460–6468.
- [21] S. Khelili, P. Lebrun, P. de Tullio, B. Pirotte, *Bioorg. Med. Chem.* **2006**, *14*, 3530–3534.

- [22] L. Matesic, N. A. Wyatt, B. H. Fraser, M. P. Roberts, T. Q. Pham, I. Greguric, *J. Org. Chem.* **2013**, *78*, 11262–11270.
- [23] T. Cuvigny, C. Herve du Penhoat, M. Julia, *Tetrahedron*. **1986**, *42*, 5321–5328.
- [24] L. R. Domingo, M. J. Aurella, P. Pérez, *RSC Adv.* **2014**, *4*, 16567–16577.
- [25] J. Soto-Delgado, J. A. Sáez, R. A. Tapia, L. R. Domingo, *Org. Biomol. Chem.* **2013**, *11*, 8357–8365.
- [26] L. R. Domingo, S. R. Emamian, *Tetrahedron*. **2014**, *70*, 1267–1273.
- [27] L. R. Domingo, P. Pérez, J. A. Sáez, *Org. Biomol. Chem.* **2012**, *10*, 3841–3851.
- [28] D. Yepes, J. S. Murray, P. Pérez, L. P. Domingo, P. Politzer, P. Jaque, *Phys. Chem. Chem. Phys.* **2014**, *16*, 6726–6734.
- [29] M. P. Uliana, B. M. Servilha, O. Alexopoulos, K. T. de Oliveira, C. F. Tormena, M. A. B. Ferreira, T. J. Brocksom, *Tetrahedron*. **2014**, *70*, 6963–6973.
- [30] J. Ammera, H. Mayr, *J. Phys. Org. Chem.* **2013**, *26*, 956–969.
- [31] H. Mayr, A. R. Ofial, *J. Phys. Org. Chem.* **2008**, *21*, 584–595.
- [32] H. Mayr, A. R. Ofial, *Pure Appl. Chem.* **2005**, *77*, 1807–1821.
- [33] H. Mayr, B. Kempf, A. R. Ofial, *Acc. Chem. Res.* **2003**, *36*, 66–77.
- [34] S. V. Bondarchuk, B. F. Minaev, *J. Phys. Chem. A*. **2014**, *118*, 3201–3210.
- [35] S. V. Bondarchuk, B. F. Minaev, *Chem. Phys. Lett.* **2014**, *607*, 75–80.
- [36] S. V. Bondarchuk, B. F. Minaev, A. Yu. Fesak, *Int. J. Quantum Chem.* **2013**, *113*, 2580–2588.
- [37] F. Martinelli, A. Palmieri, M. Petrini, *Phosphorus, Sulfur, and Silicon*. **2011**, *186*, 1032–1045.
- [38] B. S. Thyagarajan, B. F. Wood Jr., *Phosphorus and Sulfur*. **1987**, *33*, 87–98.
- [39] K. L. Stensaas, B. V. McCarty, N. M. Touchette, J. B. Brock, *Tetrahedron*. **2006**, *62*, 10683–10687.
- [40] Y. Zhu, H.-T. Tang, Z.-P. Zhan, *Adv. Synth. Catal.* **2013**, *355*, 1291–1296.
- [41] M. J. Duer, The basics of solid-state NMR, in: *Solid-state NMR Spectroscopy Principles and Applications* (Eds: M. J. Duer), Blackwell Science Ltd, Oxford, **2001**.
- [42] A. O. Bryhas, V. S. Matyichuk, T. Lis, V. Kinzhybalov, V. V. Smalius, M. D. Obushak, *Tetrahedron Lett.* **2013**, *54*, 5667–5670.
- [43] R. G. Parr, L. von Szentpály, S. Liu, *J. Am. Chem. Soc.* **1999**, *121*, 1922–1924.
- [44] R. G. Parr, R. A. Donnelly, M. Levy, W. E. Palke, *J. Chem. Phys.* **1978**, *68*, 3801–3807.
- [45] R. G. Parr, R. G. Pearson, *J. Am. Chem. Soc.* **1983**, *105*, 7512–7516.
- [46] L. R. Domingo, P. Pérez, *Org. Biomol. Chem.* **2011**, *9*, 7168–7175.
- [47] The experimental IE of tetracyanoethylene is available from NIST Chemistry Book Web site.
- [48] C. Hansch, A. Leo, R. W. Taft, *Chem. Rev.* **1991**, *91*, 165–195.
- [49] S. V. Bondarchuk, B. F. Minaev, *J. Phys. Chem. A*. **2014**, *118*, 8872–8882.
- [50] S. V. Bondarchuk, B. F. Minaev, *J. Phys. Org. Chem.* **2014**, *27*, 640–651.
- [51] R. F. W. Bader, *Atoms in Molecules. A Quantum Theory*, Clarendon, Oxford, **1990**.
- [52] P. Sjöberg, J. S. Murray, T. Brinck, P. Politzer, *Can. J. Chem.* **1990**, *68*, 1440–1443.
- [53] H. Jacobsen, *Can. J. Chem.* **2008**, *86*, 695–702.
- [54] B. Silvi, A. Savin, *Nature*. **1994**, *371*, 683–686.
- [55] J. Poater, M. Solà, M. Duran, X. Fradera, *Theor. Chem. Acc.* **2002**, *107*, 362–371.
- [56] E. Matito, J. Poater, M. Solà, M. Duran, P. Salvador, *J. Phys. Chem. A*. **2005**, *109*, 9904–9910.
- [57] F. Feixas, E. Matito, J. Poater, M. Solà, *J. Phys. Chem. A*. **2011**, *115*, 13104–13113.
- [58] M. D. Obushak, M. B. Lyakhovych, M. I. Ganushchak, *Tetrahedron Lett.* **1998**, *39*, 9567–9570.
- [59] Y. V. Ostapiuk, M. D. Obushak, V. S. Matyichuk, M. Naskrent, A. K. Gzella, *Tetrahedron Lett.* **2012**, *53*, 543–545.
- [60] N. T. Pokhodylo, V. S. Matyichuk, M. D. Obushak, *Tetrahedron*. **2009**, *65*, 2678–2683.
- [61] M. D. Obushak, V. S. Matyichuk, V. V. Turytsya, *Tetrahedron Lett.* **2009**, *50*, 6112–6115.
- [62] S. V. Bondarchuk, B. F. Minaev, *Chem. Phys.* **2011**, *389*, 68–74.
- [63] S. V. Bondarchuk, B. F. Minaev, *J. Mol. Struct. (THEOCHEM)*. **2010**, *952*, 1–7.
- [64] B. F. Minaev, S. V. Bondarchuk, M. Gıṙtu, *J. Mol. Struct. (THEOCHEM)*. **2009**, *904*, 14–20.
- [65] B. F. Minaev, S. V. Bondarchuk, *Russ. J. Appl. Chem.* **2009**, *82*, 840–845.
- [66] B. F. Minaev, S. V. Bondarchuk, A. Yu. Fesak, *Russ. J. Appl. Chem.* **2010**, *83*, 36–43.
- [67] Ö. Rubio-Pons, O. Loboda, B. Minaev, B. Schimmelpfennig, O. Vahtras, H. Ågren, *Mol. Phys.* **2003**, *101*, 2103–2114.
- [68] S. V. Bondarchuk, B. F. Minaev, *RSC Adv.* **2015**, *5*, 11558–11569.
- [69] V. M. Naidan, V. V. Smalius, *Russ. J. Gen. Chem.* **2004**, *74*, 1386–1388.
- [70] M. J. Frisch, G. W. Trucks, H. B. Schlegel, G. E. Scuseria, M. A. Robb, J. R. Cheeseman, G. Scalmani, V. Barone, B. Mennucci, G. A. Petersson, H. Nakatsuji, M. Caricato, X. Li, H. P. Hratchian, A. F. Izmaylov, J. Bloino, G. Zheng, J. L. Sonnenberg, M. Hada, M. Ehara, K. Toyota, R. Fukuda, J. Hasegawa, M. Ishida, T. Nakajima, Y. Honda, O. Kitao, H. Nakai, T. Vreven, J. A. Montgomery, J. E. Peralta Jr, F. Ogliaro, M. Bearpark, J. J. Heyd, E. Brothers, K. N. Kudin, V. N. Staroverov, R. Kobayashi, J. Normand, K. Raghavachari, A. Rendell, J. C. Burant, S. S. Iyengar, J. Tomasi, M. Cossi, N. Rega, J. M. Millam, M. Klene, J. E. Knox, J. B. Cross, V. Bakken, C. Adamo, J. Jaramillo, R. Gomperts, R. E. Stratmann, O. Yazyev, A. J. Austin, R. Cammi, C. Pomelli, J. W. Ochterski, R. L. Martin, K. Morokuma, V. G. Zakrzewski, G. A. Voth, P. Salvador, J. J. Dannenberg, S. Dapprich, A. D. Daniels, O. Farkas, J. B. Foresman, J. V. Ortiz, J. Cioslowski, D. J. Fox, *Gaussian 09*, Revision A.02 Gaussian, Inc., Wallingford, CT, **2009**.
- [71] W. Kohn, L. Sham, *Phys. Rev. A* **1965**, *140*, A1133–A1138.
- [72] A. D. Becke, *J. Chem. Phys.* **1993**, *98*, 5648–5652.
- [73] C. Lee, W. Yang, R. G. Parr, *Phys. Rev. B* **1988**, *37*, 785–789.
- [74] W. J. Hehre, L. Radom, P. v. R. Schleyer, J. A. Pople, *Ab Initio Molecular Orbital Theory*, Wiley, New York, **1986**.
- [75] R. Krishnan, J. S. Binkley, R. Seeger, J. A. Pople, *J. Chem. Phys.* **1980**, *72*, 650–654.
- [76] S. Miertuš, E. Scrocco, J. Tomasi, *Chem. Phys.* **1981**, *55*, 117–129.
- [77] T. A. Keith, AIMAll, version 10.07.25, T. K. Gristmill Software, Overland Park, KS, **2010**.
- [78] T. Lu, F. Chen, *J. Comput. Chem.* **2012**, *33*, 580–592.
- [79] F. de Proft, C. Van Alsenoy, A. Peeters, W. Langenaeker, P. Geerlings, *J. Comput. Chem.* **2002**, *23*, 1198–1209.
- [80] *Materials Studio 5.5*, Accelrys, Inc., San Diego, CA, **2008**.
- [81] A. Klamt, G. Schüürmann, *J. Chem. Soc., Perkin Trans.* **1993**, *2*, 799–805.

## SUPPORTING INFORMATION

Additional supporting information may be found in the online version of this article at the publisher's website.